Current Applied Physics 11 (2011) S12–S16

Contents lists available at ScienceDirect

Current Applied Physics

journal homepage: www.elsevier.com/locate/cap

Influence of hydrogen plasma treatment on Al-doped ZnO thin films for amorphous silicon thin film solar cells

Fang-Hsing Wang*, Hung-Peng Chang, Chih-Chung Tseng, Chia-Cheng Huang, Han-Wen Liu

Department of Electrical Engineering and Graduate Institute of Optoelectronic Engineering, National Chung Hsing University, 250 Kuo-Kuang Rd., Taichung 402, Taiwan, ROC

ARTICLE INFO

Article history:
Received 7 September 2010
Received in revised form
29 November 2010
Accepted 29 November 2010
Available online 4 December 2010

Keywords:
Al-doped ZnO (AZO)
RF magnetron sputter
H_2 plasma treatment
Silicon thin film solar cell
Plasma-enhanced CVD (PECVD)

ABSTRACT

This study investigates the effects of H_2 plasma treatment on characteristics of Al-doped ZnO (AZO) thin films prepared by RF magnetron sputter at 200 °C for amorphous silicon (α-Si) thin film solar cell fabrication. Results of X-ray diffraction analysis showed that the structure of the plasma-treated film did not change but its crystallinity deteriorated as compared to that of the as-deposited film. The electrical resistivity of the AZO films decreased after H_2 plasma treatment, regardless of plasma power. The most improvements in the electrical and optical properties of the AZO film were obtained by applying H_2 plasma RF power of 50 W, where the film resistivity decreased from 1.23×10^{-3} to 8.23×10^{-4} Ω cm and the average optical transmittance in the wavelength range of 400–700 nm increased slightly from 89.5% to 91.7%. To enhance light trapping in solar cells, surface-textured AZO films were developed using diluted HCl etching and the haze ratio beyond 30% was obtained. Additionally, the α-Si thin film solar cells consisting of the prepared AZO thin film as the transparent electrodes were fabricated. The efficiency of the cell increased form 3.26% for the as-deposited AZO film to 5.14% for the 0.2%-HCl-etched and H_2 plasma-treated film.

1. Introduction

Transparent conductive oxide (TCO) thin films are widely used for opto-electronic device applications, such as solar cells, flat panel displays, gas sensors, and low emissivity windows [1–8]. Nowadays, indium-tin-oxide (ITO) films are the most used TCO films for displays and solar cells in industry. However, a shortage of indium may occur in the future because of the limited nature of world indium reserves. Therefore, it is important to survey candidates like tin oxide (SnO_2) and zinc oxide (ZnO) films. ZnO has an n-type wide bandgap with a wurtzite crystal structure. Conductivity of an undoped ZnO thin film is determined by its native defects mainly including oxygen vacancies and zinc interstitials [2]. However, the conductivity of undoped ZnO films is not high enough for contact layer application in thin film solar cells and is not very stable at high temperatures [9]. Therefore, ZnO films are doped to enhance further their conductivity and stability using dopants such as aluminum, gallium, indium, etc. [4,10]. In particular, aluminum-doped ZnO (AZO) films have been widely investigated in recent years because of their comparable high optical transmittance, low electrical resistivity, as well as good stability in hydrogen plasma [11,12].

Researchers have employed many deposition techniques to prepare ZnO-based thin films, including molecular beam epitaxy (MBE) [13], pulsed laser deposition (PLD) [14], sol-gel method [15], chemical vapor deposition (CVD) [16], spray pyrolysis method [17] and DC/RF magnetron sputtering [18–22]. Among these processes, RF magnetron sputtering is one of the most promising method for depositing ZnO thin films owing to the inherent ease with which the deposition conditions can be controlled well [8].

To enhance properties of ZnO-based films, some post-treatment techniques have been studied [11,23,24]. Oh et al. [11] and Fang et al. [23] reported the effects of post-deposition annealing in vacuum and in an H_2 ambient on the electrical properties of AZO thin films. Strzhemechny et al. [24] described that remote plasma hydrogenation could increase electron concentrations in ZnO single crystals. The post-deposition treatment of TCO films using plasma-enhanced CVD (PECVD) is more convenient and practical for large-area applications such as thin film solar cells and has been demonstrated as to enhance the electrical properties of AZO thin films [25].

Silicon thin film solar cells in the *p-i-n* superstrate structure require TCO films as transparent electrodes, which should combine low electrical resistivity and high optical transparency in the required spectral range. Sputtering technique usually yields flat

* Corresponding author. Tel.: +886 4 22840688x706; fax: +886 4 22851410.
E-mail address: fansen@dragon.nchu.edu.tw (F.-H. Wang).

1567-1739/$ – see front matter
doi:10.1016/j.cap.2010.11.109

AZO thin films. However, a suitable textured surface is very important to scatter an incident light, particularly the long wavelength light (red and near-infrared), to extend the effective path length within the active silicon layer and subsequent light trapping inside the absorber material of the solar cell [26]. Wet chemical etching of AZO films has been adopted to develop the textured surface for enhancing the efficiency of solar cells [3].

This study investigated the structural, electrical, and optical properties of AZO thin films deposited by RF magnetron sputtering and post-treated by H_2 plasma at various RF powers. Besides, the effects of diluted hydrochloric acid (HCl) etching on surface morphology of AZO thin films and the characteristics of amorphous silicon (α-Si) thin film solar cells fabricated using the prepared AZO films as front electrodes were explored.

2. Experiments

AZO thin films were deposited on glass substrates (Coning 1737) using RF magnetron sputtering with a target consisted of 98 wt% ZnO and 2 wt% Al_2O_3. The substrates with an area of 33 × 33 mm^2 were cleaned with isopropyl alcohol (IPA) and deionized (DI) water, and then dried under blown nitrogen gas. The base pressure was 5×10^{-6} Torr and the working pressure was 5×10^{-3} Torr. The deposition temperature was at 200 °C. The as-deposited AZO films were then treated by H_2 plasma at 200 °C for 30 min in a typical PECVD chamber. To acquire textured AZO films, wet etching was performed in diluted HCl with concentrations of 0.1%, 0.2%, and 0.5% in H_2O. Afterward, *p-i-n* α-Si:H thin film solar cells were fabricated using PECVD on the textured AZO film coated glass substrates at a temperature of 200 °C. An Al layer was thermally evaporated as back electrodes of solar cells.

Film thickness was measured by a spectroscopic ellipsometer (Nano-view SE, MF-1000). The resistivity, Hall mobility, and carrier concentration were measured using a four-point probe apparatus (Napson, RT−70/RG−5) and the Van der Pauw method (BIO-RAD, HL5500IU). X-ray diffraction (XRD) (PANalytical, 18 kW rotating anode x-ray generator) analysis was employed to evaluate film structure. Surface morphology was observed by a field emission scanning electron microscope (FE-SEM) (JEOL, JSM-6700). Optical transmittance was measured as the transmittance ratio of a film coated substrate relative to an uncoated substrate by a UV/VIS/NIR spectrophotometer (Jasco, V-570). Current−voltage characteristics of solar cells were measured under an illumination intensity of 300 mW/cm^2 and an AM 1.5 G spectrum. All measurements were performed at room temperature.

3. Results and discussion

3.1. Structural, electrical, and optical properties of plasma-treated AZO thin films

Sputtered AZO thin films with a thickness of 330 nm are prepared to study the effects of post-treatments on the characteristics of the films. Fig. 1 shows the XRD data of the AZO thin films treated at different H_2 plasma RF powers. All the AZO films had a strong (0 0 2) peak at $2\theta \sim 34.31°$, indicating a preferential c-axis orientation perpendicular to the substrate with a hexagonal wurtzite structure. The peak intensity of the plasma-treated film decreased, revealing deteriorated crystal quality due to hydrogen incorporation into the films during post-treatment. Besides, it was found that the full width at half-maximum (FWHM) of the (0 0 2) peak increased slightly with increasing H_2 plasma RF power. The increase in FWHM corresponds to the decrease in crystallite size as deduced from Scheer equation [27]. The observation from FS-SEM

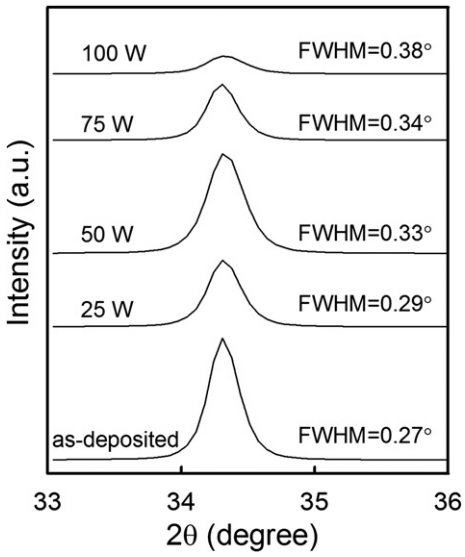

Fig. 1. XRD spectra of the AZO thin films treated with different H_2 plasma RF power.

(not shown here) also exhibits the similar trend that surface grain size decreases gradually with increasing H_2 plasma RF power.

Fig. 2 shows the resistivity, Hall mobility, and carrier concentration of the AZO thin films as a function of H_2 plasma RF power. The film resistivity showed a tendency to decrease after H_2 plasma. The resistivity decreased form 1.23×10^{-3} Ω-cm for the as-deposited films to 8.23×10^{-4} Ω-cm for the 50 W-plasma-treated films. In addition, the carrier concentration increased with increasing RF power. The Hall mobility increased first at the low RF power (25 W) and then tended to decrease at the high RF powers (≧50 W). However, the variations in the carrier concentration and Hall mobility for various plasma-treated films were not obvious. The improved electrical properties are due to not only the desorption of negatively charged oxygen species from grain boundary surfaces [23] but incorporated hydrogen atoms as shallow donors by the H_2 plasma treatment [24,28,29]. In addition, the passivation of surface and defects at grain boundaries, which diminishes scattering and trapping of free carriers and enhances the doping effect of Al, also contributes to the conductivity of the film [11]. Oh et al. [11,23] reported that hydrogen annealing treatment caused desorption of negatively charged oxygen species and passivation of film surfaces of

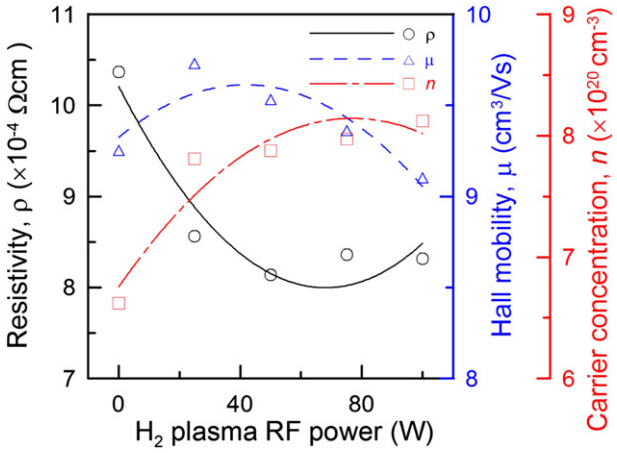

Fig. 2. Resistivity, Hall mobility, and carrier concentration of the AZO thin films as a function of H_2 plasma RF power.

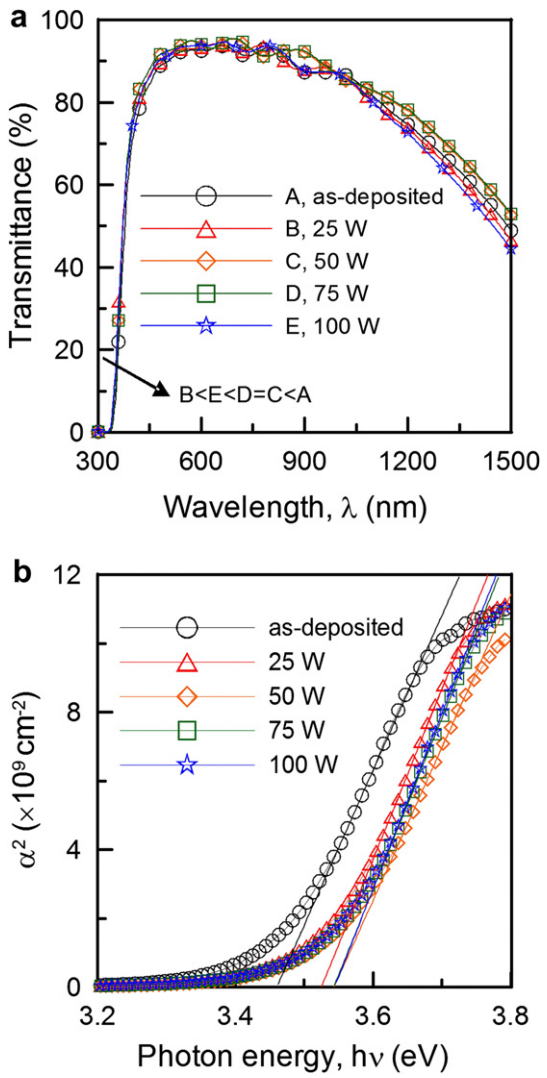

Fig. 3. (a) Optical transmittance spectra and (b) optical bandgap of the AZO thin films treated with different H_2 plasma RF power.

grain boundaries, thus improving the electrical properties and stability of AZO films. Van de Walle [28] indicated that hydrogen was a donor source in ZnO films and Hofmann et al. [29] proved the point experimentally. The secondary ion mass spectrometry (SIMS) analysis (not shown here) shows that the increased hydrogen content in the plasma-treated film may support the mechanism.

Fig. 3(a) and (b) show the optical transmittance spectra and energy bandgap of the AZO thin film treated at various H_2 plasma RF powers. For transmission measurement, the AZO thin films were irradiated at a perpendicular angle of incidence with glass being the reference. The average optical transmittance (T) of the plasma-treated films in the visible wavelength range (400–700 nm) was more than 90% while the highest T was obtained at RF powers of 50–75 W, as Table 1 lists. In the ultraviolet range, all the films exhibited a sharp absorption edge that was due to the onset of fundamental absorption of ZnO. The absorption edge slightly shifted to the lower wavelength side after H_2 plasma treatment.

Table 1
Average optical transmittance (T) and optical bandgap (E_g) of the AZO films treated at various H_2 plasma RF power.

	As-dep.	25 W	50 W	75 W	100 W
T (%)	89.5	90.4	91.7	91.7	90.8
E_g (eV)	3.462	3.525	3.542	3.542	3.542

The absorption coefficient, α, can be calculated from the relation [30]:

$$T = (1-R)^2 \exp(-\alpha d) \quad (1)$$

where T and R are the transmittance and reflectance of films, and d is the film thickness. The optical bandgap is determined by applying the Tauc model, and the Davis and Mott model in the high absorption region [30]:

$$\alpha h\nu = C(h\nu - E_g)^{1/2} \quad (2)$$

where $h\nu$ is the photon energy, E_g is the optical bandgap, and C is the constant. E_g can be calculated by plotting $(\alpha h\nu)^2$ vs. $h\nu$ and by extrapolating the linear portion of the absorption edge to find the intercept with energy axis, as Fig. 3(b) exhibits. E_g of the AZO thin films shifted from 3.462 eV to above 3.525 eV after H_2 plasma treatment, as Table 1 lists. The broadened E_g may result from the increase in carrier concentration. This can be explained by the Burstein-Moss effect [31], which specifies the bandgap increases with increasing carrier concentration.

For the application as the transparent electrodes of solar cells, the films must have low resistivity and high optical transparency. A way for evaluating this compromise is by means of figure of merit (*FOM*). *FOM* defined by Haacke [32] is one of the important indices for judging the effectiveness of different processes. *FOM* is defined by:

$$FOM = T^{10}/R_S \quad (3)$$

where T is the average visible transmittance and R_S is the sheet resistance of films. Fig. 4 exhibits *FOM* of the developed AZO thin films. *FOM* of all the plasma-treated films significantly increased, revealing that the H_2 plasma treatment was an effective technique to enhance the opto-electrical properties of AZO thin films. The films treated at an RF power of 50 W had the highest *FOM*. Thereby, the following study on HCl etching and thin film solar cells will adopt this plasma condition (50 W).

3.2. Surface morphology of diluted HCl-etched AZO thin films

To obtain textured AZO films, diluted HCl etching was carried out at room temperature. Fig. 5(a–d) displays the SEM images of the AZO thin films with and without HCl etching. The surface of the as-deposited film exhibited a relatively smooth granular structure, as Fig. 5(a) shows. Fig. 5 (b), (c), and (d) show the SEM images of the

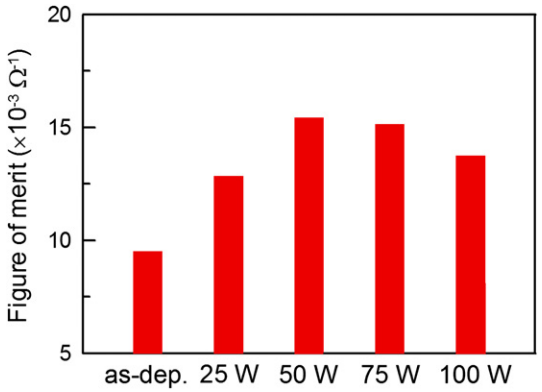

Fig. 4. Figure of merit of the AZO thin films as a function of H_2 plasma RF power.

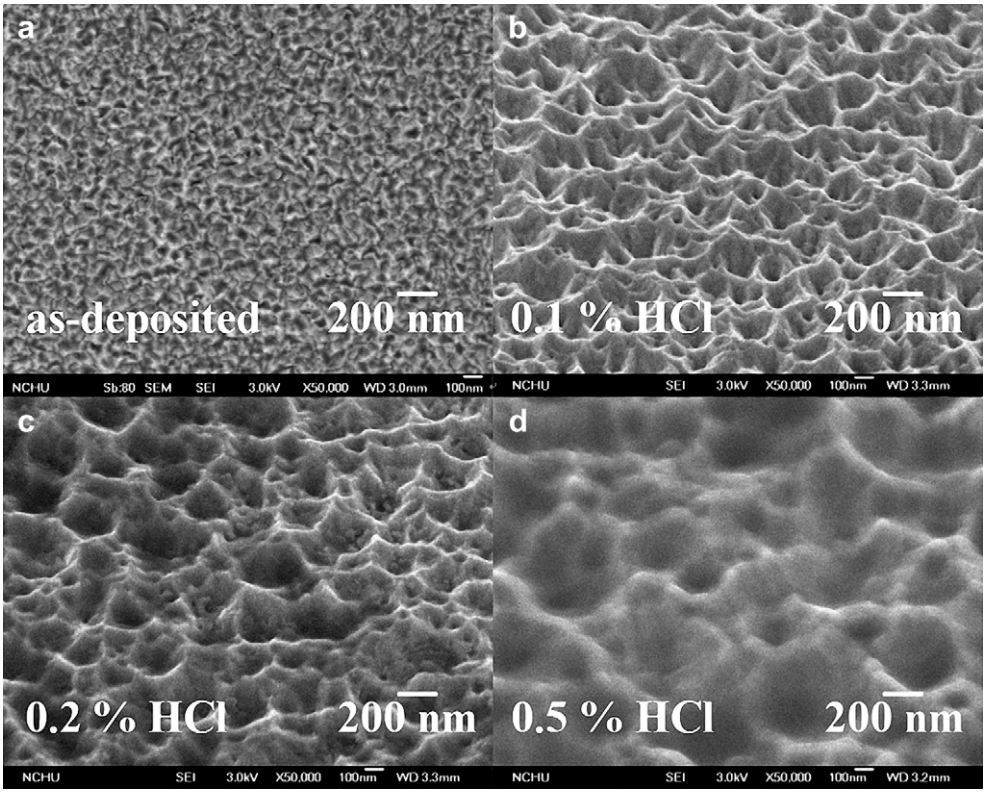

Fig. 5. SEM images of the as-deposited and the diluted HCl-etched AZO thin films.

Table 2
Sheet resistance, thickness, and haze ratio of the as-deposited and HCl-etched AZO thin films.

	Sheet resistance (Ω/□)	Film thickness (nm)	Haze ratio (%)
As-deposited	13.7	900	0.37
0.1% HCl–etched	15.6	808	22.9
0.2% HCl–etched	17.3	735	32.6
0.5% HCl–etched	26.6	491	35.1

etched films with HCl concentrations of 0.1%, 0.2%, and 0.5%, respectively, for 30 s. The surface roughness increased significantly after HCl etching and the etching caused the film surface to develop a crater-like surface structure. With increasing HCl concentration the feature size increased, but the shape of the etched surface changed from steep to flat. The haze ratio of the films before and after HCl etching was measured using a haze meter (Nippon Denshoku, NDH 2000), as Table 2 records. The sheet resistance of the etched films increased with increasing HCl concentration due to thinned film thickness. However, the haze ratio apparently increased from 0.37% (as-deposited film) to more than 30% (>0.2% HCl-etched films), revealing that the etched AZO films would effectively scatter an incident light and enhance light trapping inside the absorber material of solar cells.

3.3. Characteristics of α-Si:H thin film solar cells fabricated on the developed AZO thin film coated glass

Superstrate *p-i-n* α-Si:H thin film solar cells have been fabricated using a single-chamber PECVD at 200 °C to demonstrate the opto-electrical properties of the plasma-treated AZO film. Fig. 6 shows the structure of the superstrate *p-i-n* α-Si:H thin film solar cell. No antireflection coatings have been deposited on the cell. Fig. 7 shows the measured current–voltage characteristics of the solar cells (substrate size 3.3 × 3.3 cm^2) under illumination. Table 3 lists the values of open-circuit voltage (V_{OC}), short-circuit current density (J_{SC}), fill factor (*FF*), and efficiency (η) for the devices with the developed AZO films as the front transparent conductive films. The efficiency of the cell with the 0.2%-HCl-etched AZO film increased form 3.26% (as-deposited film) to 4.44%. Moreover, it

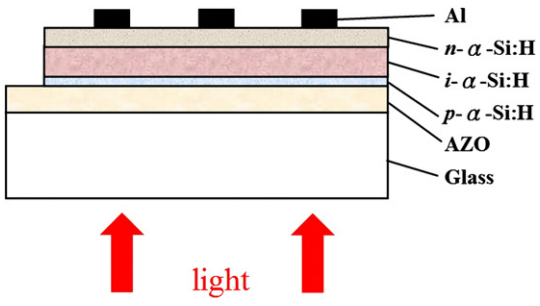

Fig. 6. Structure of the superstrate *p-i-n* α-Si:H thin film solar cell.

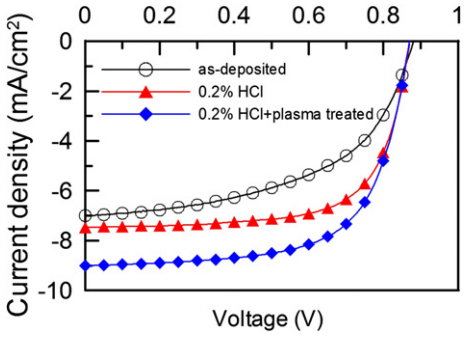

Fig. 7. Current–voltage characteristics of the *p-i-n* α-Si:H solar cells under illumination.

Table 3
Values of open-circuit voltage (V_{OC}), short-circuit current density (J_{SC}), fill factor (*FF*), and efficiency (η) for the solar cells with the as-deposited, 0.2%-HCl-etched, and H_2 plasma-treated AZO thin films.

AZO type	V_{OC} (V)	J_{SC} (mA/cm^2)	*F.F.*	η (%)
As-deposited	0.882	6.99	0.528	3.26
0.2% HCl-etched	0.872	7.47	0.682	4.44
0.2% HCl-etched + plasma-treated	0.870	9.00	0.656	5.14

could be raised to 5.14% when the AZO film was treated by H_2 plasma. The increased efficiency is mainly ascribed to the increased short-circuit current density.

4. Conclusions

The aim of this study was to study and develop AZO thin films for the application as transparent electrodes in thin film silicon solar cells. The requirements for such films are low resistivity, high transparency, and an appropriated surface structure. First, this work investigated the opto-electrical properties of AZO thin films deposited by RF magnetron sputtering and subsequently treated by H_2 plasma at various RF powers. The resistivity of the AZO film decreased by 33% (form 1.23×10^{-3} to $8.23 \times 10^{-4}\ \Omega$ cm) after the 50 W-H_2 plasma treatment. The average optical transmittances of the plasma-treated films in the visible wavelength range (400–700 nm) were over 90%. The optical bandgap of the AZO films shifted from 3.462 eV to more than 3.525 eV after H_2 plasma treatment. Upon diluted HCl etching, the AZO film developed a good surface texture and its haze ratio apparently increased from 0.37% for the as-deposited film to more than 30% for the 0.2%–0.5% HCl-etched films. Finally, the α-Si:H thin film solar cells were prepared on the developed AZO films with low resistivity, high transmittance, and good light scattering properties. The efficiency of the cell increased form 3.26% for the as-deposited AZO film to 5.14% for the 0.2%-HCl-etched and H_2 plasma-treated film. The enhanced efficiency demonstrates the potential of the H_2 plasma treatment for solar cell applications.

Acknowledgements

The authors would like to thank the National Science Council of the Republic of China, (Taiwan), for partly financially support under Contract No. NSC 95–2221–E-005–111.

References

[1] T. Söderström, F.J. Haug, X. Niquille, V. Terrazzoni, C. Ballif, Asymmetric intermediate reflector for tandem micromorph thin film silicon solar cells, Appl. Phys. Lett. 94 (2009) 063501 1–3.
[2] S. Fay, U. Kroll, C. Bucher, E. Vallat-Sauvain, A. Shah, Low pressure chemical vapour deposition of ZnO layers for thin-film solar cells: temperature-induced morphological changes, Sol. Energy Mater. Sol. Cells 86 (2005) 385–397.
[3] J. Hüpkes, B. Recha, O. Kluth, T. Repmann, B. Zwaygardt, J. Muller, R. Drese, M. Wuttig, Surface textured MF-sputtered ZnO films for microcrystalline silicon-based thin-film solar cells, Sol. Energy Mater. Sol. Cells 90 (2006) 3054–3060.
[4] J.H. Lee, Effects of hydrogen incorporation and heat treatment on the properties of ZnO: Al films deposited on polymer substrate for flexible solar cell applications, Curr. Appl. Phys. 10 (2010) S515–S519.
[5] K. Nakahara, K. Tamura, M. Sakai, D. Nakagawa, N. Ito, M. Sonobe, H. Takasu, H. Tampo, P. Fons, K. Matsubara, K. Iwata, A. Yamada, S. Niki, Improved external efficiency InGaN-based light-emitting diodes with transparent conductive Ga-doped ZnO as p-electrodes, Jan. J. Appl. Phys. 43 (2004) L180–L182.
[6] T.J. Hsueh, C.L. Hsu, S.J. Chang, I.C. Chen, Laterally grown ZnO nanowire ethanol gas sensors, Sens. Actuators, B. 126 (2007) 473–477.
[7] Z.A. Ansari, R.N. Karekar, R.C. Aiyer, Humidity sensor using planar optical waveguides with claddings of various oxide materials, Thin Solid Films 305 (1997) 330–335.
[8] Y.S. Rin, S.M. Kim, K.H. Kim, Effects of substrate heating and film thickness on properties of silver-based ZnO multilayer thin films, Jan. J. Appl. Phys. 47 (2008) 5022–5027.
[9] J. Hu, R.G. Gordon, Textured fluorine-doped ZnO films by atmospheric pressure chemical vapor deposition and their use in amorphous silicon solar cells, Solar Cells 30 (1991) 437–450.
[10] T. Minami, H. Sato, H. Nanto, S. Takata, Group III impurity doped zinc oxide thin films prepared by RF magnetron sputtering, Jpn. J. Appl. Phys. 24 (1985) L781–L784.
[11] B.Y. Oh, M.C. Jeong, J.M. Myoung, Stabilization in electrical characteristics of hydrogen-annealed ZnO: Al films, Appl. Surf. Sci. 253 (2007) 7157–7161.
[12] A.F. Aktaruzzaman, G.L. Sharma, L.K. Malhotra, Electrical, optical and annealing characteristics of ZnO: Al films prepared by spray pyrolysis, Thin Solid Films 198 (1991) 67–74.
[13] J. Hüpkes, B. Rech, S. Calnan, O. Kluth, U. Zastrow, H. Siekmann, M. Wuttig, Material study on reactively sputtered zinc oxide for thin film silicon solar cells, Thin Solid Films 502 (2006) 286–291.
[14] J.L. Zhao, X.M. Li, J.M. Bian, W.D. Yu, X.D. Gao, Structural, optical and electrical properties of ZnO films grown by pulsed laser deposition (PLD), J. Cryst. Growth 276 (2005) 507–512.
[15] K.E. Lee, M. Wang, E.J. Kim, S.H. Hahn, Structural, electrical and optical properties of sol–gel AZO thin films, Curr. Appl. Phys. 9 (2009) 683–687.
[16] D. Kim, I. Yun, H. Kim, Fabrication of rough Al doped ZnO films deposited by low pressure chemical vapor deposition for high efficiency thin film solar cells, Curr. Appl. Phys. 10 (2010) S459–S462.
[17] R. Ayouchi, D. Leinen, F. Martin, M. Gabas, E. Dalchiele, J.R. Ramos-Barrado, Preparation and characterization of transparent ZnO thin films obtained by spray pyrolysis, Thin Solid Films 426 (2003) 68–77.
[18] Y.H. Kim, K. Lee, T.S. Lee, B.k. Cheong, T.Y. Seong, W.M. Kim, Electrical, structural and etching characteristics of ZnO: Al films prepared by rf magnetron, Curr. Appl. Phys. 10 (2010) S278–S281.
[19] D.J. Kwak, J.H. Kim, B.W. Park, Y.M. Sung, M.W. Park, Y.B. Choo, Growth of ZnO: Al transparent conducting layer on polymer substrate for flexible film typed dye-sensitized solar cell, Curr. Appl. Phys. 10 (2010) S282–S285.
[20] S.H. Lee, J.H. Jung, S.H. Kim, D.K. Lee, C.W. Jeon, Effect of incident angle of target molecules on electrical property of Al-doped ZnO thin films prepared by RF magnetron sputtering, Curr. Appl. Phys. 10 (2010) S286–S289.
[21] K.U. Sim, S.W. Shin, A.V. Moholkar, J.H. Yun, J.H. Moon, J.H. Kim, Effects of dopant (Al, Ga, and In) on the characteristics of ZnO thin films prepared by RF magnetron sputtering system, Curr. Appl. Phys. 10 (2010) S463–S467.
[22] J. Kim, M.C. Kim, J. Yu, K. Park, H_2/Ar and vacuum annealing effect of ZnO thin films deposited by RF magnetron sputtering system, Curr. Appl. Phys. 10 (2010) S495–S498.
[23] G. Fang, D. Li, B.L. Yao, Fabrication and vacuum annealing of transparent conductive AZO thin films prepared by DC magnetron sputtering, Vacuum 68 (2003) 363–372.
[24] Y.M. Strzhemechny, H.L. Mosbacker, D.C. Look, D.C. Reynolds, C.W. Litton, N.Y. Garces, N.C. Giles, L.E. Halliburton, S. Niki, L.J. Brillson, Remote hydrogen plasma doping of single crystal ZnO, Appl. Phys. Lett. 84 (2004) 2545–2547.
[25] H.P. Chang, F.H. Wang, J.Y. Wu, C.Y. Kung, H.W. Liu, Enhanced conductivity of aluminum doped ZnO films by hydrogen plasma treatment, Thin Solid Films 518 (2010) 7445–7449.
[26] J. Krc, M. Zeman, O. Kluth, F. Smole, M. Topic, Effect of surface roughness of ZnO: Al films on light scattering in hydrogenated amorphous silicon solar cells, Thin Solid Films 426 (2003) 296–304.
[27] B.D. Cullity, Elements of X-ray Diffraction, second ed. Addison-Wesley, Reading, MA, 1978, p. 162.
[28] C.G. Van de Walle, Hydrogen as a cause of doping in zinc oxide, Phys. Rev. Lett. 85 (2000) 1012–1015.
[29] D.M. Hofmann, A. Hofstaetter, F. Leiter, H. Zhou, F. Henecker, B.K. Meyer, S.B. Orlinskii, J. Schmidt, P.G. Baranov, Hydrogen: a relevant shallow donor in zinc oxide, Phys. Rev. Lett. 88 (2002) 045504.
[30] S. Mandal, R.K. Singha, A. Dhar, S.K. Ray, Optical and structural characteristics of ZnO thin films grown by rf magnetron sputtering, Mater. Res. Bull. 43 (2008) 244–250.
[31] E. Burstein, Anomalous optical absorption limit in InSb, Phys. Rev. 93 (1954) 632–633.
[32] G. Haacke, New figure of merit for transparent conductors, J. Appl. Phys. 47 (1976) 4086–4089.